

# A Fast-Multi-Channel Sub-Millikelvin Precision Resistance Thermometer Readout Based on the Round-Robin Structure

Jiong Ding, Suijun Yang, Shuliang Ye

*Institute of Industry and Trade Measurement Technology, China Jiliang University, Xueyuan Street, No.258, 310018, Hangzhou, China, dingjiong@cjlu.edu.cn, corresponding author: Shuliang Ye, itmt\_paper@126.com*

The fast response multipoint high-precision temperature measurement is often necessary in many dynamical measurement fields and industrial applications. However, limited by the existing electric circuit architecture, either the AC or DC bridges have the shortcoming that the rates or precisions degenerate markedly in the multi-channel scanning mode. To overcome this disadvantage, a round-robin structural low-cost ratiometric resistance thermometer readout based on several commercial 32-bit sigma-delta analogue-to-digital converters ( $\Sigma$ - $\Delta$  ADCs) was presented in this article. The experimental results show that the precision of this readout corresponds to 0.1 mK at 1 Hz when sampling four channel resistors simultaneously, while the precision and rate are not degenerating with the channel number increasing. In addition, the uncertainty of the readout is investigated in this article. It shows that the presented readout can achieve an uncertainty as low as 2.1 mK at 1 Hz ( $K = 2$ ).

Keywords: Temperature metrology, resistance thermometry, round-robin structure, multi-channel scanning.

## 1. INTRODUCTION

The fast response synchronous multipoint high-precision temperature monitoring is often necessary in many metrology fields and industrial applications. For example, in the mass comparator system, the influences from the variety of the environmental temperature should be dynamically compensated in order to satisfy the low uncertainty mass dissemination requirement [1]. In thin film platinum resistance sensor fabrication, the fast-multi-channel resistance thermometer readout is required for online calibration. For the investigation of the super-cooling phenomena of electrolyte solutions, the multi-point temperatures should be recorded precisely and rapidly [2]. Moreover, in many temperature field reconstruction applications based on several thin-film resistance sensors, the high precision and fast measurement speed multi-channel thermometer readout is always needed [3]. According to the exciting current, the thermometer bridges are divided into two categories, the AC and DC bridges. The typical AC bridges are F18 and F900 from WIKA. The typical DC bridges are MI 6015T, FLUKE 1595, and MicroK 70 [4]. The AC bridges and MI 6015T are based on the transformers. They are considered as the most accurate resistance thermometer readouts. Unfortunately, their high cost, large size and low speed discourage their use in fast multi-channel high precision temperature monitoring. The DC bridges, except the MI 6015T, are mainly based on the analogue-to-digital

converter (ADC), named ratiometric resistance thermometer readout. The ratiometric resistance thermometer readout seems a possible solution for these requirements due to its low cost and high integration. However, whether the AC bridge or DC bridge, the ADC based bridge or the transformer-based bridge, its precision degenerates observably or its measurement speed reduces obviously when several channels are available. According to the above situation, developing a low-cost multi-channel resistance thermometer, which can overcome the precision degeneration or speed reduction when working in the multi-channel scanning mode, is significant in fast multipoint high-precision temperature monitoring.

With the great technology progress in noise reduction of electronic components, an increasing number of ADC based ratiometric thermometer readouts have been developed in recent years. These writings have pointed out the difficulty of obtaining precision at the sub-mK level, especially when it works in the multi-channel scanning mode. Schweiger designed a fast multi-channel precision thermometer readout with system noise less than 3 mK at 1 Hz [2]. He just copied the single channel structure eight times to extend the channel number. Smorگون designed a single channel low-cost ratiometric front end for industrial platinum resistance thermometer (PRT) applications. The equivalent temperature precision of this readout system was about 2 mK [5]. Ambrosetti developed a versatile and high-resolution readout system for resistance temperature detector (RTD). The system resolution (RMS) corresponds to 0.38 mK at 1 Hz [6].

With the ingenious design and high-quality fabrication, some well-known benchtop primary ratiometric resistance thermometer readouts, such as the Model 1595A from Fluke-Hart Scientific incorporated or MicroK 70 from ISOTECH incorporated, have the uncertainties of 0.02 mK after 1-minute moving average, approximately. They also can be easily extended to a multi-channel system with the automatically controlled switchbox. However, the extended channels always share the same ADC. When they work in the multi-channel scanning mode, more time is required to finish one cyclic measurement or the sample time for each channel should be decreased to overcome the time cost increase. This leads to the precision degenerating markedly. Actually, to accomplish several channels, measurement in one second is not available in almost all of the primary resistance thermometer readouts, because in the primary standard temperature laboratory, the fast measurement is usually not needed. In order to guarantee the accuracy, the shortest sample period for each channel is one second.

To obtain the equivalent temperature precision better than 0.1 mK at 1 Hz in multi-channel scanning mode, a commercial 32-bit  $\Sigma$ - $\Delta$  ADC based round-robin structural ratiometric resistance thermometer readout is presented in this study. Through selecting a series of low temperature coefficient resistors corresponding to a PRT at different temperature values, the performance of the precision, the linearity and the uncertainty of the presented readout were investigated by long time testing.

## 2. DESCRIPTION OF THE MULTI-CHANNEL RESISTANCE THERMOMETER READOUT

### A. The architecture of the classic ratiometric resistance thermometer readout

For the highest accuracy measurement, the four-wire PRT and four-wire standard reference resistor are essential in the ADC based ratiometric resistance thermometry. Traditionally, the current source reversing technique is employed for parasitic thermal electromotive forces (EMFs) and other systematic drift elimination [7]. The simplified schematic diagram of the single channel resistance thermometer readout is shown in Fig.1.a). A well-controlled constant direct current passes through the reference (REF) resistor and the PRT in series and develops two different voltage signals. Then, taking two pairs of readings with currents in opposite senses, the following are obtained:

$$ForwardV_{PRT} = \alpha[I_F \times R_{PRT} + EMF_1 + Drift_1] \quad (1)$$

$$ForwardV_{REF} = \alpha[I_F \times R_{REF} + EMF_2 + Drift_2] \quad (2)$$

$$BackwardV_{PRT} = \alpha[-I_B \times R_{PRT} + EMF_1 + Drift_1] \quad (3)$$

$$BackwardV_{REF} = \alpha[-I_B \times R_{REF} + EMF_2 + Drift_2] \quad (4)$$

where  $\alpha$  is the gain of the amplifier.  $I_F$  and  $I_B$  are the values of forward and backward current.  $R_{PRT}$  and  $R_{REF}$  are the value of the unknown PRT and REF resistor, respectively.  $EMF_1$  is

the parasitic thermal electromotive force between PRT and the connector.  $EMF_2$  is the parasitic thermal electromotive force between reference resistor and the connector.  $Drift_1$  is the systematic drift of the electronic circuit (including the amplifier and the ADC) when measuring the voltage of the PRT.  $Drift_2$  is the systematic drift of the electronic circuit when measuring the voltage of the REF. The average of the PRT and REF voltage values is given as:

$$V_{PRT} = ForwardV_{PRT} - BackwardV_{PRT} = \alpha[I_F + I_B] \times R_{PRT} \quad (5)$$

$$V_{REF} = ForwardV_{REF} - BackwardV_{REF} = \alpha[I_F + I_B] \times R_{REF} \quad (6)$$

Through computing the ratio of the measurement values of these average voltages by the microcontroller, the ratio of the REF resistor and PRT is obtained as the following equation:

$$M = \frac{R_{PRT}}{R_{REF}} = \frac{V_{PRT}}{V_{REF}} \quad (7)$$

The above method eliminates the sources of systematic errors like EMF, gain of amplifier, and circuit drift in resistance ratio computation. The accuracy of the temperature measurement mainly depends on the accuracy of the reference resistor [8]. However, when it extends to the multi-channel scanning mode, as shown in Fig.1.b), each channel shares the ADC through the mechanical relays. This noise of measurement system becomes larger, because the data conversion time of the ADC for each channel is reduced. Meanwhile, the common mode error generated from the CMRR (common-mode rejection ratio) of the amplifier has not been considered in the above equations. This is also a significant error in the ADC based ratiometric resistance thermometry [8].

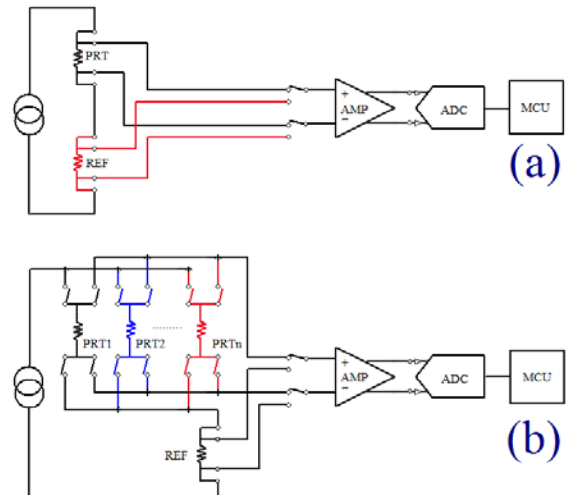


Fig.1. Topologies of ADC based ratiometric resistance thermometer readout [9]. The microcontroller controls the switchers, manages the ADC, computes the resistor's ratio, displays and sends the results. a) Classic single channel topology; b) Classic multi-channel extension topology. The combination of amplifier and ADC samples of the resistors in time-sharing mode.

### B. The architecture and measurement procedure of the presented multi-channel readout

ADC is the core component in the ratiometric resistance thermometer readout. However, the high performance and well calibrated reference resistor is the most expensive one. If we copy the single channel architecture several times to avoid the precision degeneration in multi-channel scanning mode, the price will be very high. To overcome the precision degeneration in an economical method, an architecture based on the round-robin structure, as shown in Fig.2., is studied in this article. In this architecture, a constant direct current passes through one reference (REF) resistor and  $n$  PRTs in series and develops  $n+1$  different voltage signals. Each voltage signal is amplified and sampled by the different amplifier and ADC. For ease of understanding, a two-channel round-robin architecture is selected as an example to describe the measurement procedure.

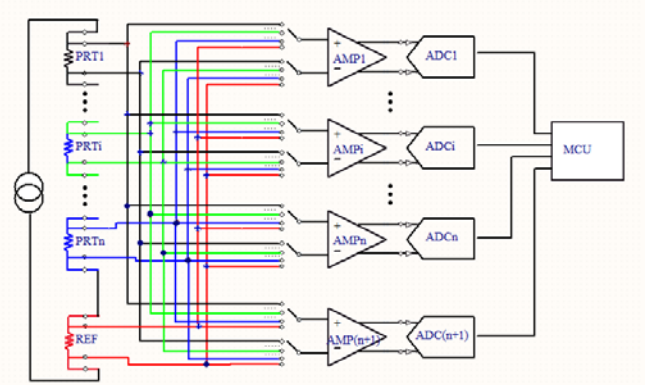


Fig.2. The architecture of the multi-channel readout based on the round-robin structure. There is one reference resistor and  $n$  PRTs,  $(n+1)$  amplifiers and ADCs. The black lines mean the signal from PRT1. The green lines mean the signal from PRT $i$ . The blue lines mean the signal from PRT $n$ . The red lines mean the signal from REF. Each amplifier and ADC combination samples every PRT and REF signal orderly according to the round-robin mechanism described in the followed paragraphs.

Step A1: the direction of the sense current is configured as forward, from the PRTs to the REF resistor. The ADC<sub>1</sub> samples the voltage from PRT<sub>1</sub>. The ADC<sub>2</sub> samples the voltage from PRT<sub>2</sub>. The ADC<sub>3</sub> samples the voltage from the REF resistor. The expressions of the input voltages of the ADCs are as follows:

$$\begin{bmatrix} FADC_{11} \\ FADC_{22} \\ FADC_{3r} \end{bmatrix} = \begin{bmatrix} (EMF_1 + Drift_1) \times \alpha_1 \\ (EMF_2 + Drift_2) \times \alpha_2 \\ (EMF_r + Drift_3) \times \alpha_3 \end{bmatrix} + \begin{bmatrix} \alpha_1 \times R_{PRT1} \times I_F \\ \alpha_2 \times R_{PRT2} \times I_F \\ \alpha_3 \times R_{REF} \times I_F \end{bmatrix} + \begin{bmatrix} \beta_1 \times \left( \frac{R_{PRT1}}{2} + R_{PRT2} + R_{REF} \right) \times I_F \\ \beta_2 \times \left( \frac{R_{PRT2}}{2} + R_{REF} \right) \times I_F \\ \beta_3 \times (R_{REF}) \times I_F \end{bmatrix} \quad (8)$$

where  $FADC_{11}$  is the voltage from PRT<sub>1</sub> sampled by ADC<sub>1</sub>.  $FADC_{22}$  is the voltage from PRT<sub>2</sub> sampled by ADC<sub>2</sub>.  $FADC_{3r}$  is the voltage from REF sampled by ADC<sub>3</sub>.  $\alpha_1$ ,  $\alpha_2$ , and  $\alpha_3$  are the differential gains of the AMP<sub>1</sub>, AMP<sub>2</sub>, and AMP<sub>3</sub>, respectively.  $\beta_1$ ,  $\beta_2$ , and  $\beta_3$  are the common gains of the AMP<sub>1</sub>, AMP<sub>2</sub>, and AMP<sub>3</sub>, respectively.  $I_F$  is the value of forward current.  $EMF_1$  and  $EMF_2$  are the parasitic thermal electromotive forces between PRT<sub>1</sub>, PRT<sub>2</sub> and their connectors, respectively.  $EMF_r$  is the parasitic thermal electromotive force between REF resistor and connector.  $Drift_1$  is the systematic voltage drift of AMP<sub>1</sub> and ADC<sub>1</sub>.  $Drift_2$  is the systematic voltage drift of AMP<sub>2</sub> and ADC<sub>2</sub>.  $Drift_3$  is the systematic voltage drift of AMP<sub>3</sub> and ADC<sub>3</sub>.

Step A2: the direction of the sense current remaining unchanged and modifying the switchers' connections between resistors and ADCs, the ADC<sub>1</sub> samples the voltage from PRT<sub>2</sub>. The ADC<sub>2</sub> samples the voltage from the REF. The ADC<sub>3</sub> samples the voltage from the PRT<sub>1</sub>. The expressions of the input voltages of the ADCs are as follows:

$$\begin{bmatrix} FADC_{12} \\ FADC_{2r} \\ FADC_{31} \end{bmatrix} = \begin{bmatrix} (EMF_2 + Drift_1) \times \alpha_1 \\ (EMF_r + Drift_2) \times \alpha_2 \\ (EMF_1 + Drift_3) \times \alpha_3 \end{bmatrix} + \begin{bmatrix} \alpha_1 \times R_{PRT2} \times I_F \\ \alpha_2 \times R_{REF} \times I_F \\ \alpha_3 \times R_{PRT1} \times I_F \end{bmatrix} + \begin{bmatrix} \beta_1 \times \left( \frac{R_{PRT2}}{2} + R_{REF} \right) \times I_F \\ \beta_2 \times \left( \frac{R_{REF}}{2} \right) \times I_F \\ \beta_3 \times \left( \frac{R_{PRT1}}{2} + R_{PRT2} + R_{REF} \right) \times I_F \end{bmatrix} \quad (9)$$

where  $FADC_{12}$  is the voltage from PRT<sub>2</sub> sampled by ADC<sub>1</sub>.  $FADC_{2r}$  is the voltage from REF sampled by ADC<sub>2</sub>.  $FADC_{31}$  is the voltage from PRT<sub>1</sub> sampled by ADC<sub>3</sub>.

Step A3: through changing the switchers' connections, the ADC<sub>1</sub> samples the voltage from REF. The ADC<sub>2</sub> samples the voltage from PRT<sub>1</sub>. The ADC<sub>3</sub> samples the voltage from PRT<sub>2</sub>. The expressions of the input voltages of the ADCs are as follows:

$$\begin{bmatrix} FADC_{1r} \\ FADC_{21} \\ FADC_{32} \end{bmatrix} = \begin{bmatrix} (EMF_r + Drift_1) \times \alpha_1 \\ (EMF_1 + Drift_2) \times \alpha_2 \\ (EMF_2 + Drift_3) \times \alpha_3 \end{bmatrix} + \begin{bmatrix} \alpha_1 \times R_{REF} \times I_F \\ \alpha_2 \times R_{PRT1} \times I_F \\ \alpha_3 \times R_{PRT2} \times I_F \end{bmatrix} + \begin{bmatrix} \beta_1 \times \left( \frac{R_{REF}}{2} \right) \times I_F \\ \beta_2 \times \left( \frac{R_{PRT1}}{2} + R_{PRT2} + R_{REF} \right) \times I_F \\ \beta_3 \times \left( \frac{R_{PRT2}}{2} + R_{REF} \right) \times I_F \end{bmatrix} \quad (10)$$

where  $FADC_{1r}$  is the voltage from REF sampled by ADC<sub>1</sub>.  $FADC_{21}$  is the voltage from PRT<sub>1</sub> sampled by ADC<sub>2</sub>.  $FADC_{32}$  is the voltage from PRT<sub>2</sub> sampled by ADC<sub>3</sub>.

Step B1: changing the direction of the sense current to the backward direction, from the REF resistor to the PRTs and modifying the switchers' connections between PRTs or REF and ADCs. The ADC<sub>1</sub> samples the voltage from PRT<sub>1</sub>. The ADC<sub>2</sub> samples the voltage from PRT<sub>2</sub>. The ADC<sub>3</sub> samples the voltage from REF resistor. The expressions of the input voltages of the ADCs are as follows:

$$\begin{bmatrix} BADC_{11} \\ BADC_{22} \\ BADC_{3r} \end{bmatrix} = \begin{bmatrix} (EMF_1 + Drift_1) \times \alpha_1 \\ (EMF_2 + Drift_2) \times \alpha_2 \\ (EMF_r + Drift_3) \times \alpha_3 \end{bmatrix} - \begin{bmatrix} \alpha_1 \times R_{PRT1} \times I_B \\ \alpha_2 \times R_{PRT2} \times I_B \\ \alpha_3 \times R_{REF} \times I_B \end{bmatrix} + \begin{bmatrix} \beta_1 \times (\frac{R_{PRT1}}{2}) \times I_B \\ \beta_2 \times (R_{PRT1} + \frac{R_{PRT2}}{2}) \times I_B \\ \beta_3 \times (R_{PRT1} + R_{PRT2} + \frac{R_{REF}}{2}) \times I_B \end{bmatrix} \quad (11)$$

where  $I_B$  is the value of backward current.  $BADC_{11}$  is the voltage from PRT<sub>1</sub> sampled by ADC<sub>1</sub>.  $BADC_{22}$  is the voltage from PRT<sub>2</sub> sampled by ADC<sub>2</sub>.  $BADC_{3r}$  is the voltage from REF sampled by ADC<sub>3</sub>.

Step B2: Through changing the switchers' connections, the ADC<sub>1</sub> samples the voltage from PRT<sub>2</sub>. The ADC<sub>2</sub> samples the voltage from REF. ADC<sub>3</sub> samples the voltage from REF. The expressions of the input voltages of the ADCs are as follows:

$$\begin{bmatrix} BADC_{12} \\ BADC_{2r} \\ BADC_{31} \end{bmatrix} = \begin{bmatrix} (EMF_2 + Drift_1) \times \alpha_1 \\ (EMF_r + Drift_2) \times \alpha_2 \\ (EMF_1 + Drift_3) \times \alpha_3 \end{bmatrix} - \begin{bmatrix} \alpha_1 \times R_{PRT2} \times I_B \\ \alpha_2 \times R_{REF} \times I_B \\ \alpha_3 \times R_{PRT1} \times I_B \end{bmatrix} + \begin{bmatrix} \beta_1 \times (R_{PRT1} + \frac{R_{PRT2}}{2}) \times I_B \\ \beta_2 \times (R_{PRT1} + R_{PRT2} + \frac{R_{REF}}{2}) \times I_B \\ \beta_3 \times (\frac{R_{PRT1}}{2}) \times I_B \end{bmatrix} \quad (12)$$

where  $BADC_{12}$  is the voltage from PRT<sub>2</sub> sampled by ADC<sub>1</sub>.  $BADC_{2r}$  is the voltage from REF sampled by ADC<sub>2</sub>.  $BADC_{31}$  is the voltage from PRT<sub>1</sub> sampled by ADC<sub>3</sub>.

Step B3: the direction of the sense current remaining the same and modifying the switchers' connections, the ADC<sub>1</sub> samples the voltage from REF. The ADC<sub>2</sub> samples the voltage from PRT<sub>1</sub>. The ADC<sub>3</sub> samples the voltage from PRT<sub>2</sub>. The expressions of the input voltages of the ADCs are as follows:

$$\begin{bmatrix} BADC_{1r} \\ BADC_{21} \\ BADC_{32} \end{bmatrix} = \begin{bmatrix} (EMF_r + Drift_1) \times \alpha_1 \\ (EMF_1 + Drift_2) \times \alpha_2 \\ (EMF_2 + Drift_3) \times \alpha_3 \end{bmatrix} - \begin{bmatrix} \alpha_1 \times R_{REF} \times I_B \\ \alpha_2 \times R_{PRT1} \times I_B \\ \alpha_3 \times R_{PRT2} \times I_B \end{bmatrix} + \begin{bmatrix} \beta_1 \times (R_{PRT1} + R_{PRT2} + \frac{R_{REF}}{2}) \times I_B \\ \beta_2 \times (\frac{R_{PRT1}}{2}) \times I_B \\ \beta_3 \times (R_{PRT1} + \frac{R_{PRT2}}{2}) \times I_B \end{bmatrix} \quad (13)$$

where  $BADC_{1r}$  is the voltage from REF sampled by ADC<sub>1</sub>.  $BADC_{21}$  is the voltage from PRT<sub>1</sub> sampled by ADC<sub>2</sub>.  $BADC_{32}$  is the voltage from PRT<sub>2</sub> sampled by ADC<sub>3</sub>.

After the switchers' connections reconfigure three times with currents in opposite senses, each ADC obtains 2×3 different voltages from every PRT and REF. The sum of the PRTs and REF voltage values in opposite senses from ADC<sub>1</sub> is:

$$V_{11} = FADC_{11} - BADC_{11} = \alpha_1 \times R_{PRT1} \times [I_F + I_B] + \beta_1 \times [(\frac{R_{PRT1}}{2} + R_{PRT2} + R_{REF}) \times I_F - \frac{R_{PRT1}}{2} \times I_B] \quad (14)$$

$$V_{12} = FADC_{12} - BADC_{12} = \alpha_1 \times R_{PRT2} \times [I_F + I_B] + \beta_1 \times [(\frac{R_{PRT2}}{2} + R_{REF}) \times I_F - (R_{PRT1} + \frac{R_{PRT2}}{2}) \times I_B] \quad (15)$$

$$V_{1r} = FADC_{1r} - BADC_{1r} = \alpha_1 \times R_{REF} \times [I_F + I_B] + \beta_1 \times [\frac{R_{REF}}{2} \times I_F - (R_{PRT1} + R_{PRT2} + \frac{R_{REF}}{2}) \times I_B] \quad (16)$$

With this procedure, the EMFs and systematic drifts are eliminated. The ratio of  $\alpha$  to  $\beta$  is the CMRR of the amplifier. It can be calibrated prior to the measuring procedure. Due to the currents in opposite directions generated from the same constant current source, the forward current  $I_F$  and backward current  $I_B$  are approximately equal. Through computing the ratio of the measurement values of these average voltages, the ratio of the PRTs and REF resistor is obtained from ADC<sub>1</sub> as the following equations:

$$M_{11} = \frac{V_{11}}{V_{1r}} = \frac{R_{PRT1} + \frac{1}{2 \times CMRR} (R_{PRT2} + R_{REF})}{R_{REF} - \frac{1}{2 \times CMRR} (R_{PRT1} + R_{PRT2})} \quad (17)$$

$$M_{12} = \frac{V_{12}}{V_{1r}} = \frac{R_{PRT2} + \frac{1}{2 \times CMRR} (-R_{PRT1} + R_{REF})}{R_{REF} - \frac{1}{2 \times CMRR} (R_{PRT1} + R_{PRT2})} \quad (18)$$

In the above equations, the  $R_{REF}$  and  $CMRR$  are the known quantities. Through the measurements, the values of  $M_{11}$  and  $M_{12}$  are obtained. The values of PRT<sub>1</sub> and PRT<sub>2</sub> can be obtained by solving these equations.

$$R_{PRT1} = \frac{4(CMRR)^2 M_{11} - 2CMRR(1 + M_{12}) + M_{11} - M_{12} + 1}{4(CMRR)^2 + 2CMRR(M_{11} + M_{12}) + M_{11} - M_{12} + 1} \times R_{REF} \quad (19)$$

$$R_{PRT2} = \frac{4(CMRR)^2 M_{12} - 2CMRR(1 + M_{11}) - M_{11} + M_{12} + 1}{4(CMRR)^2 + 2CMRR(M_{11} + M_{12}) + M_{11} - M_{12} + 1} \times R_{REF} \quad (20)$$

The ADC<sub>2</sub> and ADC<sub>3</sub> also sampled the voltages of PRT<sub>1</sub>, PRT<sub>2</sub>, and REF, respectively. According to the equations (8)-(13), the values of PRT<sub>1</sub> and PRT<sub>2</sub> can also be solved through the voltages from ADC<sub>2</sub> and ADC<sub>3</sub>. Then averaging the values of PRT<sub>1</sub> and PRT<sub>2</sub> from the three ADCs, the averaged result is obtained:

$$\overline{PRT}_i = \frac{1}{2+1} \sum_{j=1}^{2+1} PRT_{ij} \quad (21)$$

where the  $PRT_{ij}$  is the value of PRT<sub>i</sub> computed from ADC<sub>j</sub>. When the  $n$  PRTs want to be measured based on the round-robin structure, we need  $(n+1)$  ADCs. And the resistance value calculation method can be easily obtained through extending the above equations.

Compared with the single channel architecture, the major characteristic of the round-robin structure is that there are  $(n+1)$  ADCs or  $\Sigma$ - $\Delta$  engines that intersect sampling concurrently. The noise of the final result of PRT $_i$  is lower than the level from single ADC due to the parallel averaging, while the measurement speed has not declined compared with the single channel architecture. The other improvement of this measurement procedure is the common mode error correction. After CMRR correction and combining with the ADC linear calibration, the high linear performance of the resistance thermometer readout will be obtained.

### C. The CMRR calibration based on the RBC

The principle of using the resistance bridge calibrator (RBC) to estimate the linearity of the thermometer readout is the least-squares fit [10]. According to the principle, the RBC can also be used for CMRR estimation. In this study, the RBC is a set of four resistors that can be connected in different configurations to generate a total of 35 distinct resistances [11]. Putting the RBC as the PRT $_1$ , a 100  $\Omega$  high precision resistor as the PRT $_2$  in the above two-channel system, the values of the RBC can be obtained by the equation (19). According to the maximum likelihood estimation equation is as follows:

$$S^2 = \frac{1}{N - \rho} \sum_{i=1}^N (P_{i,meas} - P_{i,calc})^2 \quad (22)$$

the variance of the differences between the measured and calculated values can be calculated. Where the  $N = 35$  is the number of measured ratios.  $P_{i,meas}$  are the measured ratios calculated by equation (19).  $P_{i,calc}$  are the ratios calculated from the fitted values of RBCs.  $\rho$  is the negative number of fitted parameters. Here, it is 6 (four RBC resistances, CMRR, PRT $_2$ ). With the least-squares fit by the function *fminsearch* in Matlab, the CMRR of the AMP $_1$  can be calibrated. Meanwhile, with the same procedure, the CMRR of the AMP $_2$  and AMP $_3$  can also be calibrated.

### D. The details of key components in the multi-channel readout

The ADC, reference resistor, amplifier, and switcher are the key components of the readout system for noise and drift reduction. ADC is the kernel in ratiometric resistance thermometer readouts. With the development of digital integrated circuit design and chip manufacturing processes, the resolution of the  $\Sigma$ - $\Delta$  ADC achieved a significant progress in the recent years. In 2015, several commercial 32-bit  $\Sigma$ - $\Delta$  ADCs were available in the market. In this article, one of the available 32-bit  $\Sigma$ - $\Delta$  ADCs named AD7177-2 from Analog Device Incorporated is employed [12]. The output data rates of the AD7177-2 range from 5 samples per second (SPS) to 10,000 SPS. Its root mean square noise is lower than 0.1  $\mu$ V at 16.67 SPS. This means the effective resolution of the AD7177-2 can achieve 0.01 ppm, approximately. Meanwhile, the AD7177-2 integrates several digital filters for both the 50 Hz and the 60 Hz power line interference rejection. For each AD7177-2, like for the most of

commercial ADCs, there are several input channels, but only one  $\Sigma$ - $\Delta$  engine. In order to realize the round-robin structure, it needs  $(n+1)$  chip ADCs.

The stability and repeatability of readout depends largely on the performance of the reference resistor. The reference resistor should have low temperature coefficient and time drift. In this design, a 100  $\Omega$  ultra-high precision resistor named VHP203 from Vishay Precision Group is employed as the reference resistor [13]. With the bulk metal foil technology, hermetic sealing and oil filling, the temperature coefficient of the resistor is better than  $\pm 0.2$  ppm/K. Its shelf life stability is better than 2 ppm for at least 6 years. Its tolerance is up to  $\pm 10$  ppm. To obtain the higher temperature measurement accuracy, the reference resistor is calibrated by a direct current comparator bridge (MI 6015T) before soldering. The outcome of this calibration is 100.0002154  $\Omega$ . The uncertainty is 8.7  $\mu\Omega$  ( $k = 1$ ). Also, the designed multi-channel readout can use a high-performance external standard resistor as the reference for more accuracy requirement, such as Tinley 5685A.

Instrumentation amplifier is also the key component in the ratiometric resistance readout. Due to the tolerance of the gain resistor, the gain of each channel is different to each other. However, the gain difference and drift can be eliminated through the above mathematical analysis. The most important parameters for selecting an amplifier in the ratiometric resistance readout are the noise, distortion, and common-mode rejection ratio (CMRR). The AD8422 is a high precision, low noise, rail-to-rail instrumentation amplifier from Analog Device Incorporated [14]. Its peak-to-peak output noise is 0.15  $\mu$ V. The nonlinearity is better than 0.5 ppm. The minimum CMRR is 110 dB at Gain = 10.

Another important component in the readout is the switcher. There are two main kinds of switchers, one is mechanical relay, and the other one is CMOS multiplexer. In this design, the CMOS multiplexer ADG888 from Analog Device Incorporated is selected as the switcher between amplifier and resistor, because of its ultralow resistance distortion [15]. The reason of using the CMOS multiplexer is that it has faster response than the relay. It is suitable for rapid channel switch. The other advantage of using the CMOS multiplexer is reducing the size and power consumption of the readout. This significantly decreases the parasitic thermal EMFs on the switch.

## 3. RESULTS

### A. Noise performance estimation

To assess the noise performance of the round-robin structural resistance thermometer readout, a series of different value four-wire resistors kept in the oil bath (Fluke 7341 at 295.15 K) with a peak-to-peak stability better than 0.05 K are used in this investigation. The multi-channel readout is configured as single channel mode, double channel mode, triple channel mode, and quadruple channel mode. The whole experimental setup is shown in Fig.3. The values of the tested resistors are 50  $\Omega$ , 100  $\Omega$ , 150  $\Omega$ , and 350  $\Omega$ , respectively. In the single channel mode, each value resistor was measured independently for noise performance

estimation. In the double channel mode, the combination of 50 Ω and 100 Ω, the combination of 100 Ω and 150 Ω, the combination of 150 Ω and 350 Ω, and the combination of 50 Ω and 350 Ω were measured for noise performance estimation. In the triple channel mode, the combination of 50 Ω, 100 Ω, 150 Ω, the combination of 50 Ω, 100 Ω and 350 Ω, the combination of 50 Ω 150 Ω and 350 Ω, and the combination of 100 Ω, 150 Ω and 350 Ω were measured. In the quadruple channel mode, the combination of 50 Ω, 100 Ω, 150 Ω and 350 Ω was measured. Setting the exciting current as 1 mA (the uncertainty of the current is 15.1 nA (k = 1)) and the data out rate as 1 Hz without moving average, the standard deviation is calculated in Fig.4. for different value resistors and channel modes.

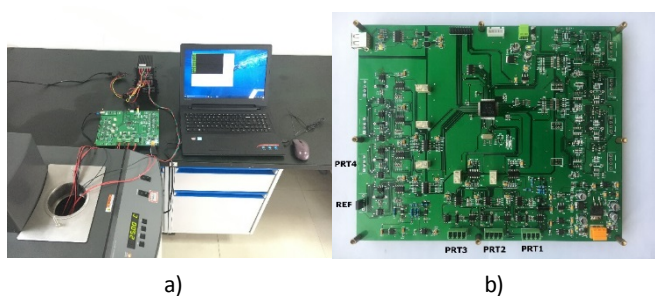


Fig.3. The photos of experimental systems. a) The tested system, including resistors, circuit, computer, power supply and oil bath. b) The photo of the designed readout.

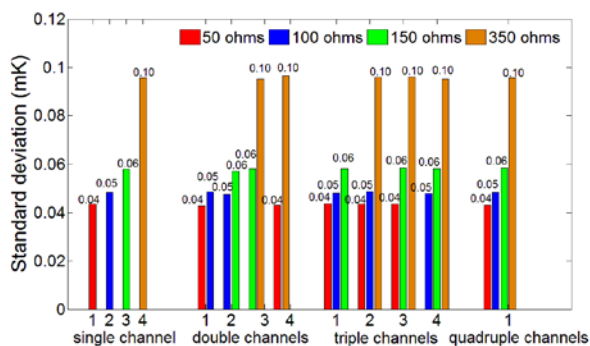


Fig.4. The noise performance of the round-robin structural readout in different channel configuration modes. There are four kinds of different value resistors in this test. It corresponds to the temperature range from 144 K to 900 K.

Almost all the primary resistance thermometers are not available in the fast scanning mode. In the article, a like-for-like comparison of the noise performance between the round-robin structural readout and a commercial portable readout, named Fluke 1529, is carried out. The Fluke 1529 is a four-channel integrating ADC based thermometry readout. Its schematic is similar to the topology shown in Fig.1.a). It can work in single channel mode, double channel mode and quadruple channel mode. Actually, Fluke 1529 cannot measure four channels in a second, because when it works in the multi-channel scan mode, the shortest sample period the user can set is 0.5 seconds. Using the Fluke 1529 to measure the above resistors, setting the exciting current as 1 mA, the

standard deviation is calculated in Fig.5. In order to keep the time for one cycle measurement equal in each mode, the sample period in the single channel mode is set as 2 second; it is set as 1 second in the double channel mode; it is set as 0.5 seconds in the quadruple channel mode.

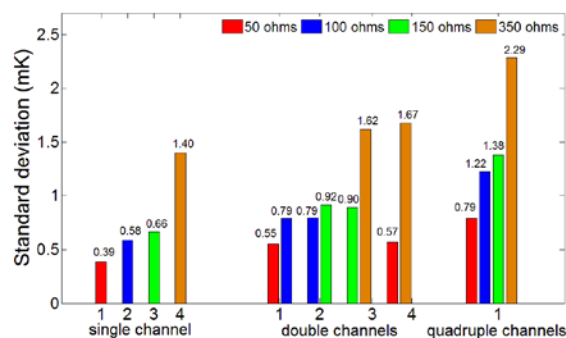


Fig.5. The noise performance of the Fluke 1529 in different channel configuration modes. The value of the internal reference resistor is 100 Ω, approximately. In the single channel mode, the integrating time of the ADC is longer than in the multi-channel scan mode through modifying the instrument configuration.

The above results show that standard deviation of the measured data is increasing with the resistor's value. In the presented readout, the precision was not degenerating with the channel number increasing. The precision and the number of channels is independent of one another. Considering the test resistor as the 100 Ω SPRT, the equivalent temperature precision of the readout achieves 0.1 mK at 1 Hz in either number of channel modes, while in the Fluke 1529, the precision degenerates with the channel number increasing. Because the Fluke 1529 uses the classic multi-channel extension topology as shown in Fig.1.b), these channels share the ADC conversion time in the multi-channel scanning mode.

Table 1. The precision comparison between designed multi-channel readout and the other classic resistance thermometers.

Bridge	Value [Ω]	Current [mA]	Average time [second]	Standard deviation [mK]
Our readout	100	1.0	32	0.020
ASL F900	100	1.0	/	0.005
FLUKE 1595A	100	1.0	30	0.010
Isotech MicroK 70	25	1.0	/	0.009
MI 6020T	100	1.0	/	0.005

In resistance thermometry, the output ratio between standard platinum resistance thermometer (SPRT) and reference resistor is always moving average for ten or sixty seconds, because the dynamic response time of the large diameter SPRT is very slow. To compare the precision with some well-known resistance bridges and ratiometric resistance thermometers, the relationship between the

precision and moving average number is estimated in the quadruple channel mode. As shown previously, the noise depends largely on the window size of moving average  $n$ . When  $n$  is set as 32, the noise performance of the designed readout is approaching several primary resistance thermometer readouts, as shown in Table 1. The data of noise performance of the well-known resistance thermometers come from their official specifications.

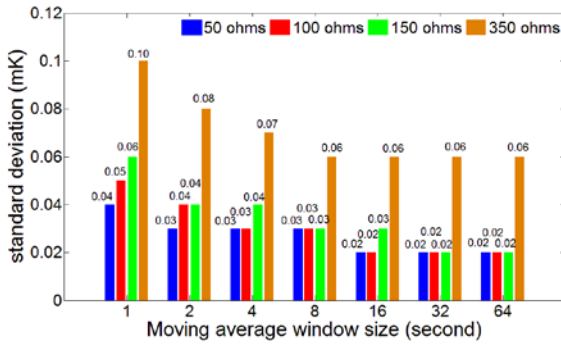


Fig.6. The standard deviation of the round-robin structural readout under different moving average window sizes.

### B. Self-heating correction and linearity evaluation

In this design, the self-heating effects are corrected by the zero-power extrapolation method. It is a mature method in the resistance thermometry field [16]. In this study, the values of the self-heating current are 1 mA and  $\sqrt{2}/2$  mA. From the self-heating correction point of view, the round-robin structure has the advantage compared to the classic multi-channel extension topology in the multi-channel mode, because in the round-robin structure, all the resistors are in series. No matter which resistor is sampled, the current heats the resistor stably. While in the classic multi-channel extension topology as shown in Fig.1.b), when one resistor is sampled, the current will not pass through the other resistors. This makes the temperature of the resistor or PRT unstable. The measurement noise becomes large.

After the self-heating and CMRR correction, the linearity of the designed multi-channel readout is evaluated using a resistance bridge calibrator (RBC). The manual RBC includes a set of four ultra-high precision resistors from Vishay Precision Group that can be configured in series or parallel combinations to produce resistances ranging from 43  $\Omega$  to 346  $\Omega$  (The nominal values of the four resistors are 77.1862  $\Omega$ , 100.0000  $\Omega$ , 129.8168  $\Omega$ , and 216.8144  $\Omega$ ). The linearity evaluation principle proposed by Dr. Rod White from Measurement Standards Laboratory of New Zealand is adopted in this investigation [16]. The RBC is connected to channel PRT<sub>1</sub> of the designed readout. The channels of PRT<sub>2</sub>, PRT<sub>3</sub>, and PRT<sub>4</sub> are connected to three precision resistors. The ratio of resistance between the calibrator and the reference resistor was measured in the quadruple channel mode. The linearity evaluation results are shown in Fig.7. The nonlinear error is smaller than 0.5 ppm in the whole range. In the ADC based resistance thermometry readout, this error mainly comes from the ADC and amplifier. However, the

total nonlinear error measured in this investigation is smaller than the nonlinear error value of the AD7177-2 and the gain nonlinearity of AD8422 in their datasheets. This is because for getting one ratio between reference resistor and PRT, the voltages sampled from the five ADCs are averaged.

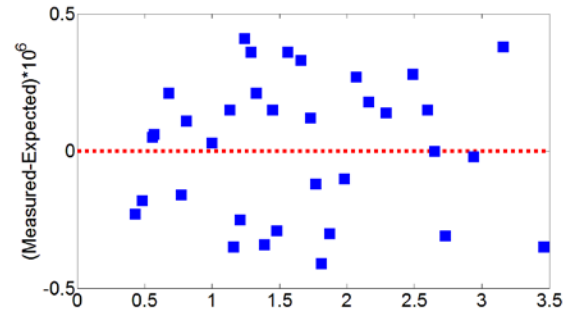


Fig.7. Residuals of nonlinearity evaluation of the designed multi-channel resistance thermometer readout.

### C. Uncertainty investigation

The uncertainty contributions of the thermometer readout are the linearity, measurement noise, and reference resistor stability [5], [17]. The uncertainty of the linearity is calculated as the largest deviation with respect to the fit line. As shown in Fig.7., the largest deviation is 0.49 ppm. The uncertainty of the measurement noise comes from the standard deviation calculated in Fig.4. The uncertainty of the reference resistor stability is calculated from the datasheet of VHP203. We assume the environment temperature range of the designed thermometer readout working is from 295.15 K to 300.15 K. The uncertainty of the reference resistor stability is 1 ppm according to the following uncertainty combination equation. The results are shown in Table 2.

$$u_o = \sqrt{\left(\frac{\partial PRT}{\partial Ratio} \times u_{Ratio}\right)^2 + \left(\frac{\partial PRT}{\partial REF} \times u_{REF}\right)^2 + (u_{linearity})^2} \quad (23)$$

Table 2. The uncertainty investigation of the multi-channel readout.

Value [ $\Omega$ ]	$u_{Ratio}$ [ppm] (k=1)	$u_{REF}$ [ppm] (k=1)	$u_{linearity}$ [ppm] (k=1)	$u_o$ [ $\mu\Omega$ ] (k=1)	Equivalent uncertainty [mK] (k=2)
50	0.15	1.00	0.49	56.84	0.30
100	0.19	1.00	0.49	112.97	0.59
150	0.23	1.00	0.49	153.52	0.80
350	0.39	1.00	0.49	391.71	2.03

The results show that the equivalent uncertainty ( $K = 2$ , at 1 Hz) of the multi-channel readout is better than 2.1 mK. Compared with some well-known primary resistance bridges, the measurement uncertainty of the multi-channel readout keeps a certain distance [18], [19]. The reason is that the temperature of the reference resistor has not been controlled

and the nonlinear of the ADCs in the designed multi-channel readout has not been well calibrated yet.

D. Temperature coefficient evaluation

Putting the designed readout in the drying oven at different temperatures, the temperature coefficient and noise performance of the readout working in the quadruple channel mode is evaluated. Setting the data out rate as 1 Hz, the noise performance at different temperatures is shown in Fig.8. The results show that the noise performance is increasing with the environmental temperature imperceptibly, due to the Johnson noise becoming larger with the temperature.

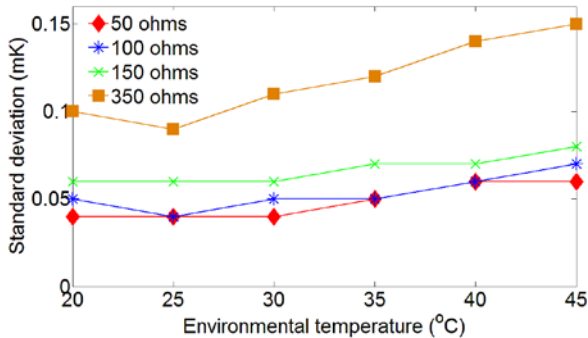


Fig.8. Standard deviation under different environmental temperatures.

Through comparison of the measured averaged ratios in 5 minutes under different environmental temperatures, the temperature coefficient of the readout is evaluated. Fig.9. shows the measuring drift under different environmental temperatures. The linear fitting result shows that the temperature coefficient of the readout is lower than 0.2 mK/K (at ratio range from 0.5 to 3.5), when the environmental temperature changes from 20 °C to 45 °C. According to the ratio measurement principle, the main contribution of the temperature coefficient of the readout comes from the reference resistor. The temperature coefficient of the VHP 203 precision resistor is lower than 0.2 ppm/K. This means the readout can adapt to some hostile industrial application environments.

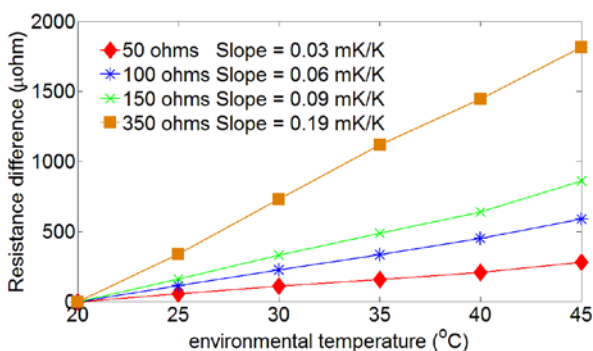


Fig.9. The temperature coefficient of the readout when measuring different value resistors.

4. DISCUSSION / CONCLUSIONS

In this article, a fast-multi-channel sub-millikelvin precision resistance thermometer readout is presented based on the round-robin structure. When it works in four channel scanning mode, the precision corresponds to 0.1 mK at 1 Hz. The overall uncertainty of the designed readout is better than 2.1 mK at 1 Hz. The main advantage of the round-robin structure is that it can avoid the precision or rate degeneration in the multi-channel scanning mode. In the round-robin architecture, for any step, each ADC samples the different PRT or reference resistor, respectively. After a whole measurement procedure, each ADC obtains the ratio between every PRT and reference resistor. Through averaging the ratio from all the ADCs, the precision of temperature measurement improves greatly.

The other advantage is the low cost of the designed multi-channel readout. Firstly, there is only one expensive reference resistor. Compared with the channel number extension through sample coping, the round-robin architecture saves the cost of multiple reference resistors. Secondly, in the designed readout, a kind of the newest commercial 32-bit  $\Sigma$ - $\Delta$  ADC is employed as the engine of the system. Typically, the integrating ADC is employed in digital multimeter and ratiometric resistance thermometer readout for a long time. However, its precision is largely limited by the clock frequency and jitter. The precision of the commercial integrating ADC is usually not higher than 24 bits. Walker uses several integrating ADCs parallelly for single channel to noise reduction in FLUKE 1595A [20]. This is contrary to the cost reduction. Bramley and Pickering developed the MicroK 70 established on a new type  $\Sigma$ - $\Delta$  ADC licensed by the National Physical Laboratory (NPL) [8]. This ADC is an application specific integrated circuit (ASIC). The manufacturing cost is not low. However, in the designed readout, we use the universal commercial ADCs. The price is just several dollars. By using this 32-bit  $\Sigma$ - $\Delta$  ADC, the precision of this readout is 0.1 mK at 1 Hz. It is close to the precision of some well-known resistance bridges.

Meanwhile, the errors generated by the CMRR of the amplifiers have been considered in this article. This error exists in all the ADC based resistance thermometer readouts. In order to reduce this error, Bramely presented a substitution topology in MicroK 70. In this topology, the PRT and the reference resistor are connected in parallel [8]. However, this topology cannot eliminate this error completely. When the difference between the PRT and reference resistor is considerable, this error cannot be ignored. In the round-robin structure, the error generated by the CMRR is larger, because all the resistors are in series. It should be considered cautiously. In this article, the CMRR of the amplifiers are calibrated first. Then, through solving the equations (19) and (20), this error is eliminated. Furthermore, distinguishing and calibrating the error from the CMRR and nonlinearity of ADC, respectively, should be adopted in ADC based

resistance thermometer readouts calibration. After CMRR and ADC calibration, the better linearity should be obtained.

#### ACKNOWLEDGMENT

This work was supported by Zhejiang Provincial Natural Science Foundation of China (Grant No. LQ15F030003, LQ17F010011), Zhejiang Key Discipline of Instrument Science and Technology (Grant No. JL150501).

#### REFERENCES

- [1] Frohlich, T., Fehling, T., Heydenbluth, D. (2009). Mass dissemination using a robot system. *tm – Technisches Messen*, 76 (7-8), 382-387.
- [2] Schweiger, H.G., Multerer, M., Gores, H.J. (2007). Fast multichannel precision thermometer. *IEEE Transactions on Instrumentation and Measurement*, 56 (5), 2002-2009.
- [3] Eke, R., Kavasoglu, A.S., Kavasoglu, N. (2012). Design and implementation of a low-cost multi-channel temperature measurement system for photovoltaic modules. *Measurement*, 45, 1499-1509.
- [4] Pearce, J.V., Gray, J., Veltcheva, R.I. (2016). Characterisation of a selection of AC and DC resistance bridges for platinum resistance thermometry. *International Journal of Thermophysics*, 37, 109.
- [5] Smorgon, D., Fericola, V.C., Coslovi, I. (2011). Low-cost ratiometric front-end for industrial PRT applications. *International Journal of Thermophysics*, 32, 2317-2324.
- [6] Ambrosetti, R., Matteoli, E., Ricci, D. (2012). Note: A versatile, stable, high-resolution readout system for RTD and thermistor sensors. *Review of Scientific Instruments*, 83, 096101.
- [7] Taylor, H.R., Navarro, H.A. (1983). A microcomputer-based instrument for applications in platinum resistance thermometry. *Journal of Physics E: Scientific Instruments*, 16, 1100-1104.
- [8] Bramley, P., Pickering, J.R. (2006). Better accuracy in temperature calibration and measurement through a new type analog-to-digital converter. *Cal Lab Magazine*, 10/11, 21-26.
- [9] Walker, R., Willgress, N. (2003). Achieving 0.25 mK uncertainty with an integrated-circuit resistance thermometer readout. In *XVII IMEKO World Congress*, Dubrovnik, Croatia, 1594-1597.
- [10] White, D.R., Williams, J.M., Ramsey I.E. (1997). A simple resistance network for the calibration of resistance bridges. *IEEE Transactions on Instrumentation and Measurement*, 42 (5), 1068-1074.
- [11] White, D.R., Clarkson, M.T., Saunders, P., Yoon, H. (2008). A general technique for calibrating indicating instruments. *Metrologia*, 45, 199-210.
- [12] Analog Devices, Inc. (2015-2016). *32-bit, 10 kSPS, Sigma-Delta ADC with 100  $\mu$ s settling and true rail-to-rail buffers*. Data Sheet AD7177-2. <http://www.analog.com/media/en/technical-documentation/data-sheets/AD7177-2.pdf>.
- [13] Vishay Precision Group. (2014). *Hermetically sealed miniature ultra high precision Z-foil technology resistors with TCR of 0.05 ppm/ $^{\circ}$ C, tolerance of  $\pm 0.001$  % and load life stability of  $\pm 0.005$  %, unaffected by humidity*. VHP203 (Z-Foil). <http://www.vishaypg.com/docs/63146/vhp203.pdf>.
- [14] Analog Devices, Inc. (2013-2015). *High performance, low power, rail-to-rail precision instrumentation amplifier*. Data Sheet AD8422. <http://www.analog.com/media/en/technical-documentation/data-sheets/AD8422.pdf>.
- [15] Analog Devices, Inc. (2005-2017). *0.4  $\Omega$  CMOS, dual DPDT switch in WLCSP/LFCSP/TSSOP*. Data Sheet ADG888. <http://www.analog.com/media/en/technical-documentation/data-sheets/ADG888.pdf>.
- [16] Nicholas, J.V., White, D.R. (2001). *Traceable Temperatures: An Introduction to Temperature Measurement and Calibration*. John Wiley & Sons.
- [17] Walker, R. (2010). Recent advances in resistance thermometry readouts. In *NCSL International Workshop and Symposium*.
- [18] Palencar, R., Sopkuliak, P., Palencar, J., Duris, S., Suroviak, E., Halaj, M. (2017). Application of Monte Carlo method for evaluation of uncertainties of ITS-90 by standard platinum resistance thermometer. *Measurement Science Review*, 17 (3), 108-116.
- [19] Duris, S., Palencar, R., Ranostaj, J. (2008). Contribution of the SPRT calibration to uncertainty of temperature T-90 measured by the calibrated SPRT. *Measurement Science Review*, 8 (1), 5-10.
- [20] Walker, R. (2011). Automatic linearity calibration in a resistance thermometry bridge. *International Journal of Thermophysics*, 32 (1-2), 215-223.

Received January 18, 2018.

Accepted July 13, 2018.